ACS APPLIED MATERIALS & INTERFACES

Research Article

Cite This: ACS Appl. Mater. Interfaces 2019, 11, 8000−8008

www.acsami.org

Strongly Coupled Phenazine−Porphyrin Dyads: Light-Harvesting Molecular Assemblies with Broad Absorption Coverage

Shin Hee Lee,[†] Adam J. Matula,[†] Gongfang Hu, Jennifer L. Troiano, Christopher J. Karpovich, Robert H. Crabtree,* Victor S. Batista,* and Gary W. Brudvig*

Department of Chemistry, and Yale Energy Sciences Institute, Yale University, New Haven, Connecticut 06520-8107, United States

Supporting Information

ABSTRACT: The development of light-harvesting architectures with broad absorption coverage in the visible region continues to be an important research area in the field of artificial photosynthesis. Here, we introduce a new class of ethynyl-linked panchromatic dyads composed of dibenzophenazines coupled *ortho* and *meta* to tetrapyrroles with an anchoring group that can be grafted onto metal oxide surfaces. Quantum chemical calculations and photophysical measurements of the synthesized materials reveal that both of the dibenzophenazine dyads absorb broadly from 300 to 636 nm and exhibit absorption bands different from those of the constituent chromophore units. Moreover, the different points of attachment of dibenzophenazines to tetrapyrroles give different absorption profiles which computations suggest result from differences in the planarity of the two dyads. Applicability of the dyads in artificial photosynthesis systems was assessed by their incorporation and characterization of their performance in dye-sensitized solar cells.

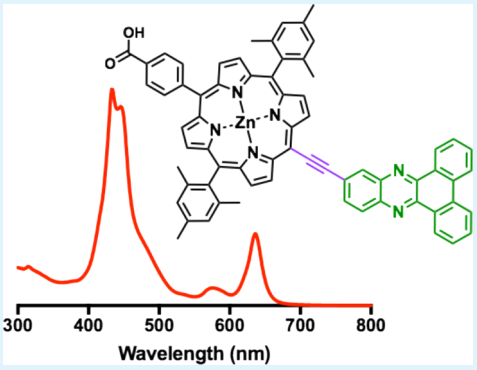

KEYWORDS: *panchromatic dyes, dyads, phenazines, porphyrins, artificial photosynthesis*

INTRODUCTION

The development of artificial photosynthetic systems could benefit from a rational design of light-harvesting molecular architectures that maximally absorb solar energy and drive chemical processes for energy conversion and storage.[1−5] Natural photosynthetic antennas often include pigments that absorb in complementary regions of the solar spectrum to achieve an overall panchromatic absorption.[6−12] Previous efforts to develop artificial panchromatic systems made use of various dyads and arrays composed of tetrapyrroles, perylenes, and polycyclic and heterocyclic aromatic hydrocarbons.[13−35] In many cases, one or more accessory chromophores or conjugated moieties were appended to a primary nonpanchromatic absorber, such as a porphyrin or a bay-annulated indigo,[36] via conjugated linkers, and the strong electronic coupling yielded absorption profiles considerably different from the sum of the spectra of the constituents chromophore units, affording strongly coupled panchromatic absorbers. Design principles have been established by comparisons of newly synthesized panchromatic dyes to well-studied dyes.[23,32,37−44] In this study, we made use of those principles to generate a list of possible phenazine-based tetrapyrrole dyad structures and identified the most promising candidates for extensive synthesis by computational screening and experimental characterizations.

Phenazines are highly conjugated heterocycles that can be structurally modified by many convenient synthetic methods.[45−53] For example, a simple condensation of *o*-phenylenediamine derivatives with functionalized *o*-quinones directly permits a variety of polyaromatic-based structures.[45,46,54] Accordingly, they are widely used as building blocks for a wide range of applications, including anticancer agents,[55−57] fluorescent markers in biological systems,[58−61] electroactive materials for organic light-emitting diodes,[50,62] organic electronics,[63] conductive polymers,[64] photoredox catalysts,[65] and as photoactive materials for photocatalysis and dye-sensitized solar cells (DSSCs).[66−70] Phenazines are particularly attractive as light-absorbing molecules because their absorption bands can be systematically tuned by increasing the number of arene rings (Figure 1). However, the majority of reported phenazines have limitations from their low extinction coefficients and their maximum absorption occurring in the green visible region. We envisioned that one route to overcome these limitations could be the attachment of porphyrins to a phenazine because porphyrins exhibit high molar extinction coefficients and feature absorption bands that stretch deeply into the red visible region. To ensure strong electronic perturbation between the phenazine and porphyrin pigments, we chose an ethynyl linker, which is widely employed in strongly coupled porphyrin architectures.[41,71−78] As expected from the strong electronic coupling between the phenazine and the porphyrin, computations show that the absorption spectra of the dyads are different from a mere sum of the spectra of the constituent fragments.

Received: November 29, 2018
Accepted: January 30, 2019
Published: January 30, 2019

DOI: 10.1021/acsami.8b20996
ACS Appl. Mater. Interfaces 2019, 11, 8000−8008

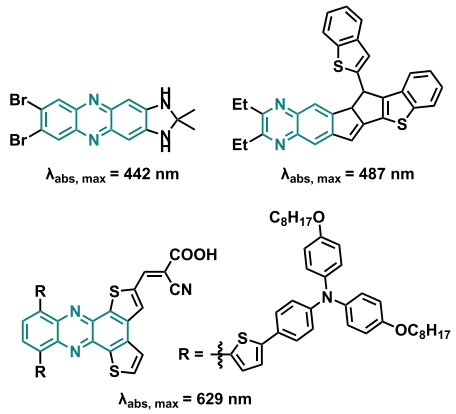

Figure 1. Examples of phenazines developed by Koepf et al.,[51] Hashmi,[5] and Zhou[79] (clockwise from top left) and their maximum absorption wavelengths.

Our work fills a gap in the existing literature by demonstrating a new class of panchromatic dyads composed of phenazines coupled to tetrapyrroles with an anchoring group that can be grafted onto metal oxide surfaces. In many other panchromatic dyad systems, the two constituent chromophores are chosen to have complementary absorption profiles, and typically both components are strongly absorbing. The phenazine used here has a low molar absorption coefficient and absorbs to the blue side of the Soret band, but it is still capable of perturbing the porphyrin's electronic structure enough to create all new bands in the red region of the visible light spectrum. By designing and synthesizing two simple dyads of this type and evaluating their potential as photosensitizers, we offer a proof-of-concept for this new class of dye, which can be further tuned with structural modifications to improve performance, opening up the design space for panchromatic dyes significantly. We thoroughly characterize the electronic and photophysical properties of these new panchromatic dyes, and we integrate them into DSSCs to characterize their performance in such systems.

RESULTS AND DISCUSSION

Molecular Design and Synthesis. The structures of phenazine−porphyrin dyads **PoZ** and **PmZ** (Schemes 1 and 2) were generated using literature-supported design principles that include: (1) the creation of an extended π-conjugation system to broaden and red-shift the absorption bands,[80,81] (2) the reduction of the symmetry of a tetrapyrrole unit to accomplish the same effect as the previous principle, (3) the use of the more electron-rich *meso*-site of the porphyrins for dye linkage to afford greater panchromaticity than would be achieved using the β-site,[23,80] (4) the use of an ethynyl linker and coplanar constituents to maximize orbital mixing and thus electronic communication,[41,71−78] and (5) the use of one large constituent rather than a number of smaller chromophore constituents, which has been more effective in broadening the absorption bands of a dye.[80] For many of the design principles, we used density functional theory (DFT)-calculated UV−vis spectra to verify their applicability to our specific systems.

Each of the dyads has a dibenzophenazine connected either *ortho* or *meta* to a zinc tetrapyrrole via an ethynyl linker at one meso position, two mesityl groups attached to meso positions of the tetrapyrrole *trans* to each other, and a phenyl linker ending in a carboxylic acid at the fourth meso position. The unfunctionalized dibenzophenazine explored in our studies is expected to foreshadow the properties of other dibenzophenazines derivatives to be the subject of future studies. Because of the vulnerability of dibenzophenazines to $\pi-\pi$ stacking, mesityl groups were appended to the tetrapyrrole core to prevent this via steric repulsion, thereby increasing solubility. The tetrapyrrole unit was selected for use in constructing an elongated π-conjugation system with the dibenzophenazines because of its ready structural flexibility and strong absorption profile which extends out to the red visible region. Tetrapyrroles also possess multiple available substitution positions that allowed our design described above, as well as the appendage of the anchoring carboxylic acid group, an essential component of many photosensitizers. The different structural configurations of our dyads (*ortho* vs *meta*) were prepared as a case study on the effects of substitution on panchromaticity; our DFT calculations indicated that while **PmZ** has a planar geometry as its minimum energy conformation, **PoZ**'s preferred conformation has a 23° dihedral angle between **Po** and the tetrapyrrole core for steric reasons (Figure S6). As the aggregation of photosensitizers is a known cause of low photovoltaic device efficiencies,[44] we explored whether the nonplanarity of **PoZ** could result in overall better photosensitizing abilities than those of **PmZ**.

The syntheses of the phenazine−porphyrin dyads were based on palladium- and copper-catalyzed Sonogashira coupling of ethynyl phenazines and bromo porphyrins.[82] Our bromo porphyrin, **4**, is a *trans*-A_2BC-porphyrin bearing two mesityl groups and a 4-carboxyphenyl group. Porphyrin **3**, the precursor porphyrin for all porphyrin derivatives discussed in this study, was prepared via a condensation reaction of dipyrromethane and mesitaldehyde in the presence of ethanol and $BF_3{\cdot}OEt_2$ followed by oxidation with DDQ.[83] The ethanol proved essential for a successful synthesis of the porphyrin.[84] Scheme 2 shows the condensed syntheses of benchmark porphyrin **AZ** and dyads **PmZ** and **PoZ**. The three steps required for generating **4** from **3** are described in the Supporting Information. They involve the selective bromination of **3** for the Suzuki coupling with methylbenzoate, followed by a bromination of **HZ** at the unsubstituted meso porphyrin site and zinc metalation with anhydrous zinc acetate to provide **4** in 91% yield. All porphyrins were preserved as esters until the final synthetic step in order to avoid unwanted side reactions.

Scheme 1. Syntheses of Ethynyldibenzophenazines

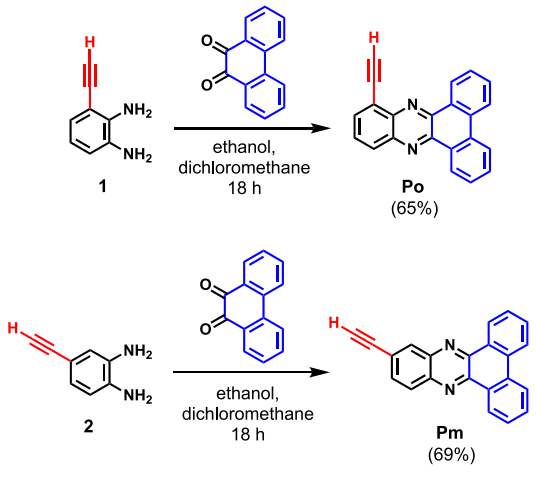

DOI: 10.1021/acsami.8b20996
ACS Appl. Mater. Interfaces 2019, 11, 8000−8008

Scheme 2. Syntheses of Phenazine–Porphyrin Dyads[a]

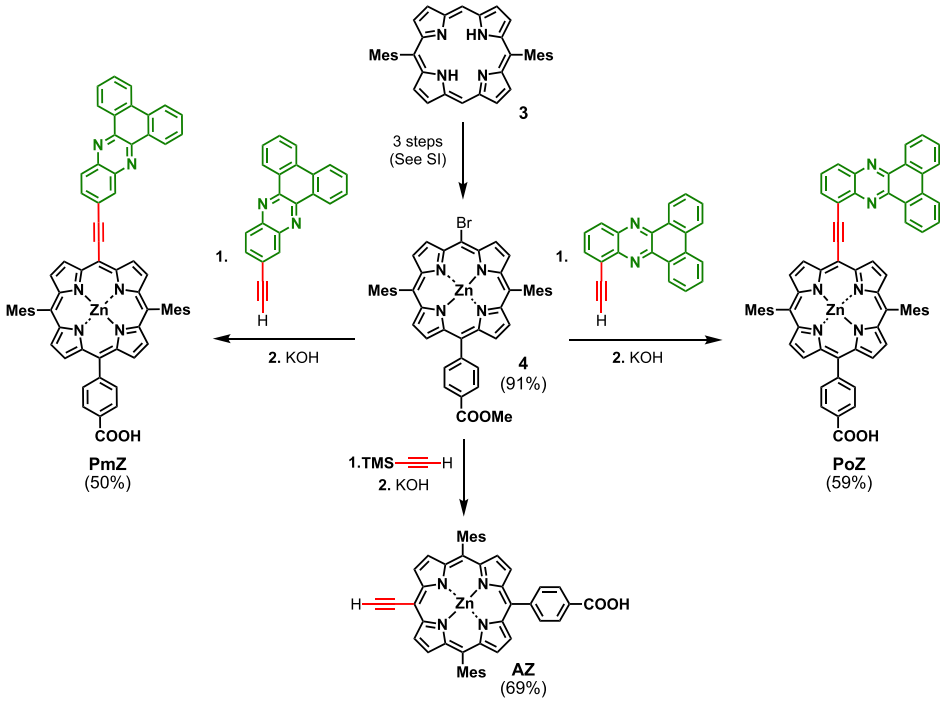

[a]Reagents and conditions: **AZ**: Zn–bromoporphyrin (1 equiv), $Pd(PPh_3)_2Cl_2$ (25% mol), CuI (25% mol), trimethylsilylacetylene (20 equiv), triethylamine (30% of solvent), THF, −7 °C to room temp, 12 h. **PmZ** and **PoZ**: Zn–bromoporphyrin (1 equiv), ethynyldibenzophenazine (3 equiv), $Pd_2(dba)_3$ (30% mol), CuI (5% mol), P(*o*-tol)$_3$ (2.4 equiv), triethylamine (20% of solvent), THF, 60 °C, overnight.

The syntheses of phenazines **Po** and **Pm** are described in Scheme 1, and the syntheses of diamines **1** and **2** are detailed in the Supporting Information. Our synthetic route deviates slightly from a reported procedure for the preparation of diethynylphenazines[48] in that we couple ethnylbenzene-1,2-diamines bearing no protecting groups with quinone derivatives. Condensation of phenanthrene-9,10-dione and ethynylbenzene-1,2-diamine in the presence of ethanol and dichloromethane afforded **Po** and **Pm** in 65 and 69% yields, respectively. The average yield for each synthetic step in the preparation of **Pm** was higher than the corresponding step of **Po**.

Hydrolysis of the intermediate dyad esters with potassium hydroxide at room temperature afforded **PmZ** and **PoZ** in yields of 50 and 59%, respectively. Sonogashira coupling of ethynyltrimethylsilane and **4**, followed by a concurrent deprotection of trimethylsilyl and hydrolysis in the presence of potassium hydroxide, provided **AZ** in 69% yield.

Quantum Chemical Calculations. Potential panchromatic dyad candidates for synthesis and experimental characterization were identified by using DFT calculations to obtain optimized molecular structures and simulated UV–vis spectra. Examining the orbitals involved in the calculated transitions also provided a detailed analysis of the origin of panchromaticity at the electronic level. In dyad systems with strong electronic coupling between the constituent chromophore units, desirable strong electronic transitions in the red (600–800 nm) region of the visible light spectrum resulted from the frontier orbitals of the system delocalized across the extended conjugated π-system of two dye moieties. Figure 2 and Figure S5 underscore this point by showing natural transition orbital (NTO) projections for the relevant transitions in both **PmZ** and **PoZ**, respectively, showing that they involve orbitals spanning the two moieties.

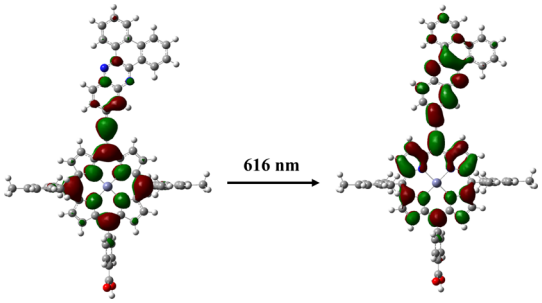

Figure 2. Calculated transition at 616 nm for **PmZ** in its minimum-energy conformation.

Accordingly, where the goal is to design a dye that absorbs across a broad region of the solar spectrum, it is important to maximize the electronic interaction of the two dye components by making use of a fully conjugating bridging group such as an ethynyl, as also demonstrated by other groups.[85] However, a variation in the degree of conjugation through the bridging group could tune the position of the red-most electronic transition. As a proof of principle, we evaluated five linker groups that connect phenazines with tetrapyrroles with varying degrees of conjugation, as well as their direct linkage. The DFT UV–vis spectra of these species (Figure 3) show that the red-most absorption peak blue-shifts and decreases in intensity as the conjugation between the two constituents decreases, from extensively conjugated ethynyl and vinyl linkers to weakly conjugated amidyl linkers. Because the ethynyl linker group offered the most promise for a panchromatic dye species, it was

DOI: 10.1021/acsami.8b20996
ACS Appl. Mater. Interfaces 2019, 11, 8000–8008

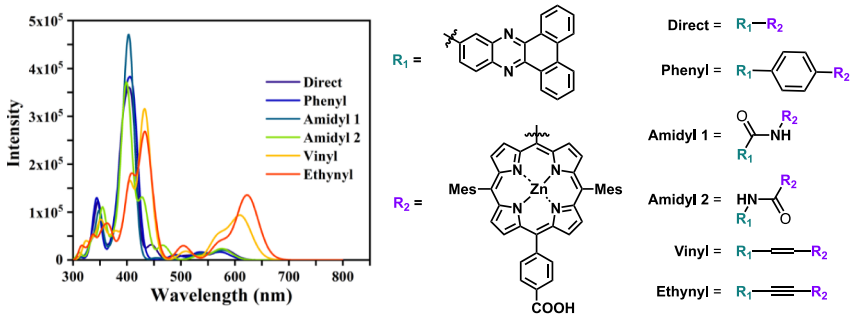

Figure 3. DFT-calculated UV−vis spectra of dyads with varying linkers in their minimum-energy conformations.

selected for use in synthesis and experimental characterization as described in the molecular design section.

For dyad **PoZ**, the calculated minimum energy non-planar conformation involves a dihedral angle of 23° between the phenazine and the tetrapyrrole. Because planarity is directly related to conjugation, it was initially assumed that **PoZ** would exhibit substantially less panchromaticity than **PmZ**. However, the ethynyl linker permits rotation, allowing the dihedral angles to vary without too great a loss of conjugation. Others have shown that it is important to take into account viable rotations when computing the absorption profile of dyes.[86] The rotational barriers of dyads **PmZ** and **PoZ** were calculated to be 1.35 and 1.70 kcal/mol, respectively (Figure S2). These relatively low barriers permit many conformations of these dyads to contribute at room temperature under a Boltzmann distribution, influencing the average overall conjugation through the molecule and the UV−vis spectra. Computing the UV−vis spectra of these dyads in different conformations and combining them via their Boltzmann yields give better relative intensities of the peaks. Figure 4 shows simulated UV−

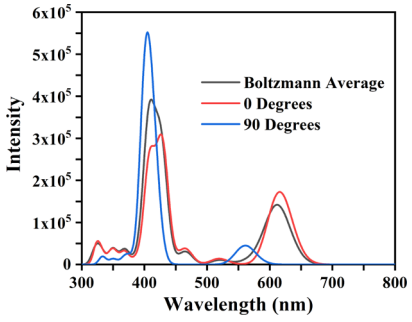

Figure 4. DFT-calculated UV−vis spectra of **PmZ** in the planar minimum-energy conformation, with a 90° dihedral angle, and Boltzmann averaged across all rotational conformations.

vis spectra with Boltzmann-averaged conformations for dyad **PmZ**. Similar results for **PoZ** and the calculated spectra of **HZ** and **AZ** can be found in the Supporting Information (Figures S3 and S4). Notably, the rotation about the ethynyl triple bonds substantially reduces the intensity of the red-most visible electronic transition due to the contributions of less-conjugated conformations. This suggests that a similar dyad with full-conjugation and limited rotations could possess greater panchromatic absorption.

Photophysical and Electrochemical Properties. The electronic absorption spectra of phenazines **Po** and **Pm**, dyads **PmZ** and **PoZ**, as well as that of benchmark porphyrin **AZ**, are shown in Figure 5 and the data are tabulated in Table 1. The

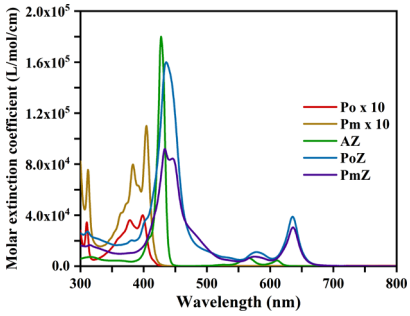

Figure 5. Absorption spectra of the phenazine and porphyrin derivatives **Po**, **Pm**, **AZ**, **PmZ**, and **PoZ** collected in anhydrous methanol and toluene, respectively, at room temperature. The molar extinction coefficients of the phenazine **Po** and **Pm** are amplified 10 times in intensity for clear comparison. The emission spectra were recorded with excitation wavelengths noted in Table S2.

Table 1. Absorption Features of the Dyads and Benchmark Compounds

compound	λ_{abs} (nm)[a]	ε_{max} ($\times 10^5$ $M^{-1}\cdot cm^{-1}$)[b]	$FWHM_{Soret}$ (cm^{-1})[c]
PmZ	434, 446, 576, 636	0.92	2018
PoZ	434, 578, 636	1.6	1743
AZ	428, 566, 611	1.8	655
Pm	312, 383, 404	0.11	
Po	310, 378, 398	0.040	

[a]Absorption spectra and molar absorption coefficients were measured in methanol at room temperature with absorbance around 1. [b]Molar absorption coefficient of the peak with the maximum absorbance. [c]Full width at half-maximum of Soret bands of porphyrins.

absorption spectrum of benchmark porphyrin **HZ** and emission spectra of **Po**, **Pm**, **AZ**, **PmZ**, and **PoZ** are displayed in the Supporting Information (Figure S1). The overlaid spectra reveal that the absorptions of **PmZ** and **PoZ** are not linear sums of those of the constituents **Pm**, **Pm**, **AZ**, and **HZ**; each exhibits new absorption peaks that are not observed for the constituents. The new peak at 640 nm is much more intense ($\varepsilon \approx 3.0 \times 10^4$ $M^{-1}\cdot cm^{-1}$) and red-shifted relative to the Q-bands in the monomeric porphyrins ($\lambda_{abs} \approx 610$ nm, $\varepsilon \approx 0.50 \times 10^4$ $M^{-1}\cdot cm^{-1}$) as a result of the conjugation of the phenazine and porphyrin derivatives. This underscores the existence and importance of strong electronic coupling between the two dyes through the ethynyl linker. Having a lower extinction coefficient but more similar intensities of the Soret and Q-bands, the phenazine−porphyrin dyad **PmZ** exhibits better orbital mixing and panchromaticity than **PoZ**. However, the wavelengths of the maximum absorptions and

DOI: 10.1021/acsami.8b20996
ACS Appl. Mater. Interfaces 2019, 11, 8000−8008

emissions are unaffected by the position of the ethynyl group (*ortho* vs *meta*) with respect to the zinc porphyrin, and the two dyads exhibit an almost identical absorption maximum wavelength in the red region. The integration of a phenazine moiety on one side of the molecule decreases the symmetry of the porphyrin macrocycle, resulting in less-degenerate B_x and B_y states and broader Soret bands in the porphyrin−phenazine dyads compared to those of the monomeric porphyrin **AZ**. The noncoplanar conformation of **PmZ** affords even less-degenerate B states than in its counterpart **PoZ**, as shown by a larger spectral splitting in the Soret region. Importantly, both of the dyads demonstrate nonzero absorption from the near-ultraviolet to near-infrared regions (i.e., panchromatic absorption) which is apparent when compared to the absorption profile of the ethynylporphyrin **AZ**.

The molecular structures of **PmZ-Ester**, **PoZ-Ester**, and **AZ-Ester**, which are ester versions of the **PmZ**, **PoZ**, and **AZ**, are shown in the Supporting Information, as well as the cyclic voltammogram of **HZ-Ester**. As seen in Figure 6, the cyclic

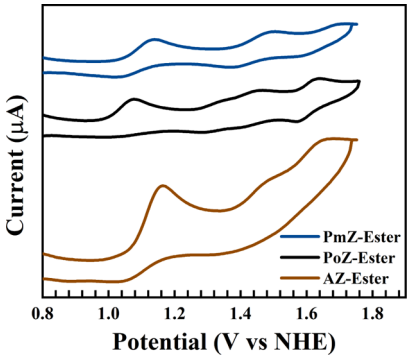

Figure 6. Cyclic voltammograms of **AZ-Ester**, **PoZ-Ester**, and **PmZ-Ester** in 0.1 M $TBAPF_6$ in dichloromethane with a 50 mV/s scan rate.

voltammograms of **AZ-Ester** and **PoZ-Ester** exhibit pronounced irreversibility of the first oxidation feature, whereas that of **PmZ-Ester** exhibits only mild irreversibility of this same feature. The loss of the return feature suggests that a chemical change may be taking place upon oxidation, likely involving the ethynyl group. Ethynyl groups have high acidity and reactivity, which are further increased under these oxidizing conditions.[85] The increased reversibility of **PmZ-Ester** as compared to **PoZ-Ester** could in part be explained by the structure and conjugation of the molecules. The minimum energy conformation of **PoZ-Ester** is nonplanar with a dihedral angle of 23°; however, it is completely planar for **PmZ-Ester**. This causes the ethynyl group of **PoZ-Ester** to be more similar to that of **AZ-Ester** and, therefore, more susceptible to a chemical reaction. **PmZ-Ester**, alternatively, has a minimum energy conformation with increased conjugation between the porphyrin and the phenazine due to its planarity, shifting the electronic properties of the ethynyl group. To probe when the chemical change may take place, the potential window was narrowed to 1.25 V versus NHE, but the irreversibility remained. This indicates that if a chemical change does occur, it happens at or near the potential of the first oxidation feature.

Photovoltaic Performance. The performances of TiO_2-based photovoltaic devices with photosensitizers **HZ**, **AZ**, **PmZ**, and **PoZ** were measured under standard conditions (AM 1.5G, 100 mW/cm^2) using iodine/triiodide (I^-/I_3^-) liquid electrolyte. Additional photovoltaic parameters are summarized in Table 2; MK-2 was used as a reference cell and its overall efficiency of 4.97 ± 0.25 agreed closely with the literature.[87] The phenazine−porphyrin dyads **PoZ** and **PmZ** perform better than the benchmark porphyrins **HZ** and **AZ** as expected given their panchromatic absorption (Figure 7). Of

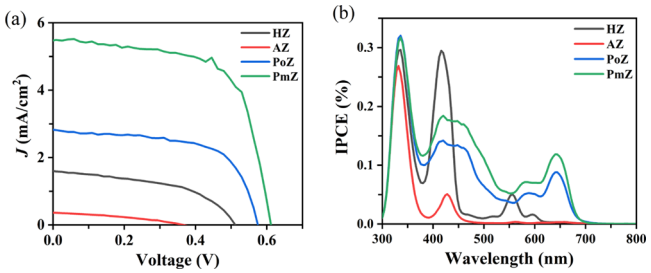

Figure 7. (a) Current density vs voltage (J−V) curve and (b) incident photon to current efficiency (IPCE) profile of devices with photosensitizers **HZ**, **AZ**, **PoZ**, and **PmZ**.

the two dyads, **PmZ** performed the best, affording an open-circuit photovoltage (V_{oc}) of 0.61 V, a short-circuit photocurrent density (J_{sc}) of 5.47 mA/cm^2, a fill factor (ff) of 0.68, and an overall solar-to-electrical energy conversion efficiency (η) of 2.29%. Additionally, the device with **PmZ** exhibited a higher surface coverage of dye molecules, which could be a result of the increased planarity of **PmZ**, allowing more photosensitizers access to the TiO_2 surface. While performing other optimizations of the devices would likely improve their efficiencies, the focus of this study is on the electronic and photophysical properties of the dyes, not on the optimization of photovoltaic devices.

CONCLUSIONS

We have prepared two bichromophoric phenazine−porphyrin dyads and evaluated their photophysical, electrochemical, and photovoltaic properties. We predetermined the structures of the dyads with suitable absorption profiles from quantum chemistry calculations. Calculations of the absorption spectra of dibenzophenazine connected to a tetrapyrrole with a variety of linkers showed that the ethynyl linker gave the broadest absorption coverage because of the stronger electronic coupling between the two constituent dyes. The dyads, synthesized via a Sonogashira coupling of ethynyl phenazines and bromoporphyrins, showed absorption extending from 300 to 636 nm. The reported results demonstrate that the conjugated linkage of phenazines and tetrapyrroles yields

Table 2. Photovoltaic Parameters for Photosensitizers HZ, AZ, PoZ, and PmZ

cell specification	V_{oc} (V)	J_{sc} (mA/cm^2)	ff (%)	η (%)	dye surface coverage (mM/cm^2)	η (%)/dye surface coverage
HZ	0.52 ± 0.02	1.60 ± 0.22	0.56 ± 0.08	0.47 ± 0.12	0.037	12.7
AZ	0.39 ± 0.05	0.36 ± 0.09	0.40 ± 0.19	0.06 ± 0.05	0.024	2.5
PoZ	0.57 ± 0.01	2.58 ± 0.49	0.63 ± 0.06	0.94 ± 0.19	0.039	24.1
PmZ	0.61 ± 0.01	5.47 ± 0.60	0.68 ± 0.02	2.29 ± 0.27	0.074	31.0

DOI: 10.1021/acsami.8b20996
ACS Appl. Mater. Interfaces 2019, 11, 8000−8008

panchromatic absorption, paving the way for the rational design of improved panchromatic dyads.

EXPERIMENTAL SECTION

Synthesis. The syntheses of molecules are described in the Supporting Information.

Absorption and Emission. UV−visible spectrophotometry was performed using a Shimadzu UV-2600 spectrophotometer coupled with UVProbe software. Sample solutions were carried in 1 cm × 1 cm quartz cuvettes to measure the steady-state absorption spectra and molar extinction coefficients. A detailed procedure for measuring molar extinction coefficients is described in the Supporting Information.

Electrochemistry. Cyclic voltammetry (CV) experiments were conducted using a Pine WaveNow potentiostat. A glassy carbon working electrode, an Ag/AgCl wire pseudoreference electrode, and a platinum wire counter electrode made up the three-electrode electrochemical cell. The glassy carbon working electrode was polished with an alumina slurry on a polishing pad before each experiment. The supporting electrolyte was 0.1 M tetrabutylammonium hexafluorophosphate ($TBAPF_6$), recrystallized twice prior to use, in anhydrous dichloromethane. To establish the potential of the pseudoreference electrode, the ferrocenium/ferrocene redox couple was used as an internal standard. All CVs were referenced to NHE using the measured ferrocenium/ferrocene $E_{1/2}$, which is 0.690 V versus NHE in dichloromethane.[88] Reported CVs were performed in an electrochemical cell that had been purged with N_2, but no difference was seen in the CVs recorded under air. The porphyrin concentration was 1 mM, and a 50 mV/s scan rate was used for each reported CV.

DSSC Fabrication and Photovoltaic Measurements. The DSSCs were fabricated according to the previously reported methods and the details are described in the Supporting Information.[87] The current density−voltage (J−V) and incident photo-to-electron conversion efficiency (IPCE) data were measured using a PARSTAT 4000 potentiostat (Princeton Applied Research) and a solar simulator equipped with a 1000 W ozone-free xenon lamp and AM1.5G filter. The light intensity was calibrated with ASTM E948-09 and E1021-06 standards (Newport). Spectra of the monochromatic IPCEs for the solar cells were obtained using a Keithley 2400 source meter and custom LabView software developed by our group. The dye-loadings were measured by soaking each slide in a solution of 0.05 M NaOH in water/tetrahydrofuran/ethanol (v/v/v, 1:1:1) for 4 days, drying via rotatory evaporation, and measuring their absorption spectra in methanol. The concentrations of the solutions were calculated with experimentally determined molar extinction coefficients.

DFT Calculations. All structures studied in this manuscript were optimized using DFT at the B3LYP[89]/def2SVP[90] level using the Gaussian09 software package.[91] Frequency calculations verified that the obtained minimum energy geometry was a stationary point. Linear-response time-dependent DFT calculations[92] were performed with an implicit methanol polarizable continuum model[93] to obtain 45 lowest-energy singlet electronic transitions for each molecule. Spectra shown in the manuscript were subjected to a 0.075 eV Gaussian broadening to better match experimentally obtained spectra. Rotation barrier calculations were performed by fixing the dihedral angle between the two dyes in increments of 5° from 0 to 90° and relaxing the rest of the structure. Conformationally averaged calculated spectra were obtained by weighting the calculated spectra of each rotamer by the Boltzmann weight determined by its electronic energy relative to the minimum-energy conformation and then normalizing to 1. NTO[94] analysis was used to visualize select calculated transitions as a single pair of orbitals, an excited "particle" and an empty "hole".

ASSOCIATED CONTENT

Supporting Information

The Supporting Information is available free of charge on the ACS Publications website at DOI: 10.1021/acsami.8b20996.

Synthesis and characterization of the dyads, additional absorption and emission spectra, CV data, and details on quantum calculation results (PDF)

AUTHOR INFORMATION

Corresponding Authors

*E-mail: robert.crabtree@yale.edu. Phone: 203-200-8936 (R.H.C.).
*E-mail: victor.batista@yale.edu. Phone: 203-432-6672 (V.S.B.).
*E-mail: gary.brudvig@yale.edu. Phone: 203-432-5202 (G.W.B.).

ORCID

Adam J. Matula: 0000-0002-1241-2470
Gongfang Hu: 0000-0002-0387-9079
Robert H. Crabtree: 0000-0002-6639-8707
Victor S. Batista: 0000-0002-3262-1237
Gary W. Brudvig: 0000-0002-7040-1892

Author Contributions

†S.H.L. and A.J.M. contributed equally.

Notes

The authors declare no competing financial interest.

ACKNOWLEDGMENTS

We thank the staff at the Yale West Campus Analytical Core, and the Yale Chemical and Biophysical Instrumentation Center for their help with the instrumentations. This work was supported by the U.S. Department of Energy, Chemical Sciences, Geosciences, and Biosciences Division, Office of Basic Energy Sciences, Office of Science (grant DEFG02-07ER15909). Additional support was provided by a generous donation from the TomKat Charitable Trust. V.S.B. acknowledges computational time from NERSC and Yale HPC. A.J.M. was supported by the National Science Foundation Graduate Research Fellowship under grant no. DGE-1122492.

REFERENCES

(1) Listorti, A.; Durrant, J.; Barber, J. Solar to Fuel. *Nat. Mater.* **2009**, *8*, 929−930.
(2) Scholes, G. D.; Fleming, G. R.; Olaya-Castro, A.; van Grondelle, R. Lessons from Nature about Solar Light Harvesting. *Nat. Chem.* **2011**, *3*, 763−774.
(3) Frischmann, P. D.; Mahata, K.; Würthner, F. Powering the Future of Molecular Artificial Photosynthesis with Light-Harvesting Metallosupramolecular Dye Assemblies. *Chem. Soc. Rev.* **2013**, *42*, 1847−1870.
(4) Berardi, S.; Drouet, S.; Francàs, L.; Gimbert-Suriñach, C.; Guttentag, M.; Richmond, C.; Stoll, T.; Llobet, A. Molecular Artificial Photosynthesis. *Chem. Soc. Rev.* **2014**, *43*, 7501−7519.
(5) Sekine, K.; Stuck, F.; Schulmeister, J.; Wurm, T.; Zetschok, D.; Rominger, F.; Rudolph, M.; Hashmi, A. S. K. N-Heterocycle-Fused Pentalenes by a Gold-Catalyzed Annulation of Diethynyl-Quinoxalines and -Phenazines. *Chem.—Eur. J.* **2018**, *24*, 12515−12518.
(6) Barber, J. Photosystem II: a Multisubunit Membrane Protein that Oxidises Water. *Curr. Opin. Struct. Biol.* **2002**, *12*, 523−530.
(7) Polívka, T.; Sundström, V. Ultrafast Dynamics of Carotenoid Excited States−From Solution to Natural and Artificial Systems. *Chem. Rev.* **2004**, *104*, 2021−2072.
(8) Muh, F.; Madjet, M. E.-A.; Adolphs, J.; Abdurahman, A.; Rabenstein, B.; Ishikita, H.; Knapp, E.-W.; Renger, T. α-Helices Direct Excitation Energy Flow in the Fenna Matthews Olson Protein. *Proc. Natl. Acad. Sci. U.S.A.* **2007**, *104*, 16862−16867.

DOI: 10.1021/acsami.8b20996
ACS Appl. Mater. Interfaces 2019, 11, 8000−8008

(9) Adolphs, J.; Müh, F.; Madjet, M. E.-A.; Renger, T. Calculation of Pigment Transition Energies in the Fmo Protein. *Photosynth. Res.* **2007**, *95*, 197−209.
(10) am Busch, M. S.; Müh, F.; Madjet, M. E.-A.; Renger, T. The Eighth Bacteriochlorophyll Completes the Excitation Energy Funnel in the FMO Protein. *J. Phys. Chem. Lett.* **2011**, *2*, 93−98.
(11) Moore, G. F.; Brudvig, G. W. Energy Conversion in Photosynthesis: A Paradigm for Solar Fuel Production. *Annu. Rev. Condens. Matter Phys.* **2011**, *2*, 303−327.
(12) Hildner, R.; Brinks, D.; Nieder, J. B.; Cogdell, R. J.; van Hulst, N. F. Quantum Coherent Energy Transfer over Varying Pathways in Single Light-Harvesting Complexes. *Science* **2013**, *340*, 1448−1451.
(13) Liu, Y.; Lin, H.; Li, X.; Li, J.; Nan, H. Photoinduced Electron Transfer in Panchromatic Zinc Phthalocyanine-Azobenzene Dyad. *Inorg. Chem. Commun.* **2010**, *13*, 187−190.
(14) Rio, Y.; Seitz, W.; Gouloumis, A.; Vázquez, P.; Sessler, J. L.; Guldi, D. M.; Torres, T. A Panchromatic Supramolecular Fullerene-Based Donor-Acceptor Assembly Derived from a Peripherally Substituted Bodipy-Zinc Phthalocyanine Dyad. *Chem.—Eur. J.* **2010**, *16*, 1929−1940.
(15) Warnan, J.; Buchet, F.; Pellegrin, Y.; Blart, E.; Odobel, F. Panchromatic Trichromophoric Sensitizer for Dye-Sensitized Solar Cells Using Antenna Effect. *Org. Lett.* **2011**, *13*, 3944−3947.
(16) Bozdemir, O. A.; Erbas-Cakmak, S.; Ekiz, O. O.; Dana, A.; Akkaya, E. U. Towards Unimolecular Luminescent Solar Concentrators: Bodipy-Based Dendritic Energy-Transfer Cascade with Panchromatic Absorption and Monochromatized Emission. *Angew. Chem., Int. Ed.* **2011**, *50*, 10907−10912.
(17) Bartelmess, J.; Soares, A. R. M.; Martínez-Díaz, M. V.; Neves, M. G. P. M. S.; Tomé, A. C.; Cavaleiro, J. A. S.; Torres, T.; Guldi, D. M. Panchromatic Light Harvesting in Single Wall Carbon Nanotube Hybrids-Immobilization of Porphyrin-Phthalocyanine Conjugates. *Chem. Commun.* **2011**, *47*, 3490−3492.
(18) Nieto, C. R.; Guilleme, J.; Villegas, C.; Delgado, J. L.; González-Rodríguez, D.; Martin, N.; Torres, T.; Guldi, D. M. Subphthalocyanine-Polymethine Cyanine Conjugate: an All Organic Panchromatic Light Harvester that Reveals Charge Transfer. *J. Mater. Chem. A* **2011**, *21*, 15914−15918.
(19) Warnan, J.; Gardner, J.; Le Pleux, L.; Petersson, J.; Pellegrin, Y.; Blart, E.; Hammarström, L.; Odobel, F. Multichromophoric Sensitizers Based on Squaraine for NiO Based Dye-Sensitized Solar Cells. *J. Phys. Chem. C* **2013**, *118*, 103−113.
(20) M'Sabah, B. L.; Boucharef, M.; Warnan, J.; Pellegrin, Y.; Blart, E.; Lucas, B.; Odobel, F.; Bouclé, J. Amplification of Light Collection in Solid-State Dye-Sensitized Solar Cells *via* the Antenna Effect Through Supramolecular Assembly. *Phys. Chem. Chem. Phys.* **2015**, *17*, 9910−9918.
(21) Jradi, F. M.; O'Neil, D.; Kang, X.; Wong, J.; Szymanski, P.; Parker, T. C.; Anderson, H. L.; El-Sayed, M. A.; Marder, S. R. A Step Toward Efficient Panchromatic Multi-Chromophoric Sensitizers for Dye Sensitized Solar Cells. *Chem. Mater.* **2015**, *27*, 6305−6313.
(22) Lebedeva, M. A.; Chamberlain, T. W.; Scattergood, P. A.; Delor, M.; Sazanovich, I. V.; Davies, E. S.; Suyetin, M.; Besley, E.; Schröder, M.; Weinstein, J. A.; Khlobystov, A. N. Stabilising the Lowest Energy Charge-Separated State in a {Metal Chromophore - Fullerene} Assembly: A Tuneable Panchromatic Absorbing Donor-Acceptor Triad. *Chem. Sci.* **2016**, *7*, 5908−5921.
(23) Hu, G.; Liu, R.; Alexy, E. J.; Mandal, A. K.; Bocian, D. F.; Holten, D.; Lindsey, J. S. Panchromatic Chromophore-Tetrapyrrole Light-Harvesting Arrays Constructed from Bodipy, Perylene, Terrylene, Porphyrin, Chlorin, And Bacteriochlorin Building Blocks. *New J. Chem.* **2016**, *40*, 8032−8052.
(24) Sekita, M.; Ballesteros, B.; Diederich, F.; Guldi, D. M.; Bottari, G.; Torres, T. Intense Ground-State Charge-Transfer Interactions in Low-Bandgap, Panchromatic Phthalocyanine-Tetracyanobuta-1,3-diene Conjugates. *Angew. Chem., Int. Ed.* **2016**, *55*, 5560−5564.
(25) Mishra, R.; Regar, R.; Singhal, R.; Panini, P.; Sharma, G. D.; Sankar, J. Porphyrin Based Push-Pull Conjugates As Donors for Solution-Processed Bulk Heterojunction Solar Cells: A Case of Metal-Dependent Power Conversion Efficiency. *J. Mater. Chem. A* **2017**, *5*, 15529−15533.
(26) Tsai, M.-C.; Wang, C.-L.; Chang, C.-W.; Hsu, C.-W.; Hsiao, Y.-H.; Liu, C.-L.; Wang, C.-C.; Lin, S.-Y.; Lin, C.-Y. A Large, Ultra-Black, Efficient and Cost-Effective Dye-Sensitized Solar Module Approaching 12% Overall Efficiency under 1000 lux Indoor Light. *J. Mater. Chem. A* **2018**, *6*, 1995−2003.
(27) Fernández-Ariza, J.; Urbani, M.; Rodríguez-Morgade, M. S.; Torres, T. Panchromatic Photosensitizers Based on Push-Pull, Unsymmetrically Substituted Porphyrazines. *Chem.—Eur. J.* **2017**, *24*, 2618−2625.
(28) Kawata, T.; Chino, Y.; Kobayashi, N.; Kimura, M. Increased Light-Harvesting in Dye-Sensitized Solar Cells through Förster Resonance Energy Transfer within Supramolecular Dyad Systems. *Langmuir* **2018**, *34*, 7294−7300.
(29) Aumaitre, C.; Rodriguez-Seco, C.; Jover, J.; Bardagot, O.; Caffy, F.; Kervella, Y.; López, N.; Palomares, E.; Demadrille, R. Visible and Near-Infrared Organic Photosensitizers Comprising Isoindigo Derivatives as Chromophores: Synthesis, Optoelectronic Properties and Factors Limiting their Efficiency in Dye Solar Cells. *J. Mater. Chem. A* **2018**, *6*, 10074−10084.
(30) Desta, M. B.; Vinh, N. S.; Pavan Kumar, C.; Chaurasia, S.; Wu, W.-T.; Lin, J. T.; Wei, T.-C.; Wei-Guang Diau, E. Pyrazine-Incorporating Panchromatic Sensitizers for Dye Sensitized Solar Cells under One Sun and Dim Light. *J. Mater. Chem. A* **2018**, *6*, 13778−13789.
(31) Kabir, E.; Patel, D.; Clark, K.; Teets, T. S. Spectroscopic and Electrochemical Properties of Electronically Modified Cycloplatinated Formazanate Complexes. *Inorg. Chem.* **2018**, *57*, 10906−10917.
(32) Yuen, J. M.; Diers, J. R.; Alexy, E. J.; Roy, A.; Mandal, A. K.; Kang, H. S.; Niedzwiedzki, D. M.; Kirmaier, C.; Lindsey, J. S.; Bocian, D. F.; Holten, D. Origin of Panchromaticity in Multichromophore-Tetrapyrrole Arrays. *J. Phys. Chem. A* **2018**, *122*, 7181−7201.
(33) Liao, J.; Zhao, H.; Cai, Z.; Xu, Y.; Qin, F. G. F.; Zong, Q.; Peng, F.; Fang, Y. BODIPY-Based Panchromatic Chromophore for Efficient Organic Solar Cell. *Org. Electron.* **2018**, *61*, 215−222.
(34) Ho, P.-Y.; Mark, M. F.; Wang, Y.; Yiu, S.-C.; Yu, W.-H.; Ho, C.-L.; McCamant, D. W.; Eisenberg, R.; Huang, S. Panchromatic Sensitization with ZnII Porphyrin-Based Photosensitizers for Light-Driven Hydrogen Production. *ChemSusChem* **2018**, *11*, 2517−2528.
(35) Urbani, M.; Grätzel, M.; Nazeeruddin, M. K.; Torres, T. Meso-Substituted Porphyrins for Dye-Sensitized Solar Cells. *Chem. Rev.* **2014**, *114*, 12330−12396.
(36) He, B.; Zherebetskyy, D.; Wang, H.; Kolaczkowski, M. A.; Klivansky, L. M.; Tan, T.; Wang, L.; Liu, Y. Rational Tuning of High-Energy Visible Light Absorption for Panchromatic Small Molecules by a Two-Dimensional Conjugation Approach. *Chem. Sci.* **2016**, *7*, 3857−3861.
(37) Lin, V.; DiMagno, S.; Therien, M. Highly Conjugated, Acetylenyl Bridged Porphyrins: New Models for Light-Harvesting Antenna Systems. *Science* **1994**, *264*, 1105−1111.
(38) Imahori, H.; Matsubara, Y.; Iijima, H.; Umeyama, T.; Matano, Y.; Ito, S.; Niemi, M.; Tkachenko, N. V.; Lemmetyinen, H. Effects of *meso*-Diarylamino Group of Porphyrins as Sensitizers in Dye-Sensitized Solar Cells on Optical, Electrochemical, and Photovoltaic Properties. *J. Phys. Chem. C* **2010**, *114*, 10656−10665.
(39) Ragoussi, M.-E.; de la Torre, G.; Torres, T. Tuning the Electronic Properties of Porphyrin Dyes: Effects of *meso* Substitution on Their Optical and Electrochemical Behaviour. *Eur. J. Org. Chem.* **2013**, 2832−2840.
(40) Alexy, E. J.; Yuen, J. M.; Chandrashaker, V.; Diers, J. R.; Kirmaier, C.; Bocian, D. F.; Holten, D.; Lindsey, J. S. Panchromatic Absorbers for Solar Light-Harvesting. *Chem. Commun.* **2014**, *50*, 14512−14515.
(41) Tanaka, T.; Osuka, A. Conjugated Porphyrin Arrays: Synthesis, Properties and Applications for Functional Materials. *Chem. Soc. Rev.* **2015**, *44*, 943−969.
(42) Mandal, A. K.; Diers, J. R.; Niedzwiedzki, D. M.; Hu, G.; Liu, R.; Alexy, E. J.; Lindsey, J. S.; Bocian, D. F.; Holten, D. Tailoring

DOI: 10.1021/acsami.8b20996
ACS Appl. Mater. Interfaces 2019, 11, 8000−8008

Panchromatic Absorption and Excited-State Dynamics of Tetrapyrrole-Chromophore (Bodipy, Rylene) Arrays-Interplay of Orbital Mixing and Configuration Interaction. *J. Am. Chem. Soc.* **2017**, *139*, 17547−17564.
(43) Cheema, H.; Peddapuram, A.; Adams, R. E.; McNamara, L.; Hunt, L. A.; Le, N.; Watkins, D. L.; Hammer, N. I.; Schmehl, R. H.; Delcamp, J. H. Molecular Engineering of Near Infrared Absorbing Thienopyrazine Double Donor Double Acceptor Organic Dyes for Dye-Sensitized Solar Cells. *J. Org. Chem.* **2017**, *82*, 12038−12049.
(44) Hu, G.; Kang, H. S.; Mandal, A. K.; Roy, A.; Kirmaier, C.; Bocian, D. F.; Holten, D.; Lindsey, J. S. Synthesis of Arrays Containing Porphyrin, Chlorin, and Perylene-Imide Constituents for Panchromatic Light-Harvesting and Charge Separation. *RSC Adv.* **2018**, *8*, 23854−23874.
(45) Spicer, J. A.; Gamage, S. A.; Rewcastle, G. W.; Finlay, G. J.; Bridewell, D. J. A.; Baguley, B. C.; Denny, W. A. Bis(phenazine-1-carboxamides): Structure−Activity Relationships for a New Class of Dual Topoisomerase I/II-Directed Anticancer Drugs. *J. Med. Chem.* **2000**, *43*, 1350−1358.
(46) Vicker, N.; Burgess, L.; Chuckowree, I. S.; Dodd, R.; Folkes, A. J.; Hardick, D. J.; Hancox, T. C.; Miller, W.; Milton, J.; Sohal, S.; Wang, S.; Wren, S. P.; Charlton, P. A.; Dangerfield, W.; Liddle, C.; Mistry, P.; Stewart, A. J.; Denny, W. A. Novel Angular Benzophenazines: Dual Topoisomerase I and Topoisomerase II Inhibitors as Potential Anticancer Agents. *J. Med. Chem.* **2002**, *45*, 721−739.
(47) Bunz, U. H. F. N-Heteroacenes. *Chem.—Eur. J.* **2009**, *15*, 6780−6789.
(48) Bryant, J. J.; Zhang, Y.; Lindner, B. D.; Davey, E. A.; Appleton, A. L.; Qian, X.; Bunz, U. H. F. Alkynylated Phenazines: Synthesis, Characterization, and Metal-Binding Properties of Their Bis-Triazolyl Cycloadducts. *J. Org. Chem.* **2012**, *77*, 7479−7486.
(49) Bunz, U. H. F.; Engelhart, J. U.; Lindner, B. D.; Schaffroth, M. Large N-Heteroacenes: New Tricks for Very Old Dogs? *Angew. Chem., Int. Ed.* **2013**, *52*, 3810−3821.
(50) Gu, P.-Y.; Zhao, Y.; He, J.-H.; Zhang, J.; Wang, C.; Xu, Q.-F.; Lu, J.-M.; Sun, X. W.; Zhang, Q. Synthesis, Physical Properties, and Light-Emitting Diode Performance of Phenazine-Based Derivatives with Three, Five, and Nine Fused Six-Membered Rings. *J. Org. Chem.* **2015**, *80*, 3030−3035.
(51) Koepf, M.; Lee, S. H.; Brennan, B. J.; Méndez-Hernández, D. D.; Batista, V. S.; Brudvig, G. W.; Crabtree, R. H. Preparation of Halogenated Fluorescent Diaminophenazine Building Blocks. *J. Org. Chem.* **2015**, *80*, 9881−9888.
(52) Lorenz, R.; Kaifer, E.; Wadepohl, H.; Himmel, H.-J. Di- and Tetranuclear Transition Metal Complexes of a Tetrakisguanidino-Substituted Phenazine Dye by Stepwise Coordination. *Dalton Trans.* **2018**, *47*, 11016−11029.
(53) Sheng, J.; He, R.; Xue, J.; Wu, C.; Qiao, J.; Chen, C. Cu-Catalyzed π-Core Evolution of Benzoxadiazoles with Diaryliodonium Salts for Regioselective Synthesis of Phenazine Scaffolds. *Org. Lett.* **2018**, *20*, 4458−4461.
(54) Seillan, C.; Brisset, H.; Siri, O. Efficient Synthesis of Substituted Dihydrotetraazapentacenes. *Org. Lett.* **2008**, *10*, 4013−4016.
(55) Rewcastle, G. W.; Denny, W. A.; Baguley, B. C. Potential Antitumor Agents. 51. Synthesis and Antitumor Activity of Substituted Phenazine-1-carboxamides. *J. Med. Chem.* **1987**, *30*, 843−851.
(56) Price-Whelan, A.; Dietrich, L. E. P.; Newman, D. K. Rethinking "Secondary" Metabolism: Physiological Roles for Phenazine Antibiotics. *Nat. Chem. Biol.* **2006**, *2*, 71−78.
(57) Rohrabaugh, T. N., Jr.; Collins, K. A.; Xue, C.; White, J. K.; Kodanko, J. J.; Turro, C. New Ru(ii) Complex for Dual Photochemotherapy: Release of Cathepsin K Inhibitor and 1o2 Production. *Dalton Trans.* **2018**, *47*, 11851−11858.
(58) Phillips, T.; Haq, I.; Meijer, A. J. H. M.; Adams, H.; Soutar, I.; Swanson, L.; Sykes, M. J.; Thomas, J. A. DNA Binding of an Organic dppz-Based Intercalator. *Biochemistry* **2004**, *43*, 13657−13665.
(59) Bellin, D. L.; Sakhtah, H.; Rosenstein, J. K.; Levine, P. M.; Thimot, J.; Emmett, K.; Dietrich, L. E. P.; Shepard, K. L. Integrated Circuit-Based Electrochemical Sensor for Spatially Resolved Detection of Redox-Active Metabolites in Biofilms. *Nat. Commun.* **2014**, *5*, 3256.
(60) Humeniuk, H. V.; Rosspeintner, A.; Licari, G.; Kilin, V.; Bonacina, L.; Vauthey, E.; Sakai, N.; Matile, S. White-Fluorescent Dual-Emission Mechanosensitive Membrane Probes that Function by Bending Rather than Twisting. *Angew. Chem., Int. Ed.* **2018**, *57*, 10559−10563.
(61) Schindler, J.; Traber, P.; Zedler, L.; Zhang, Y.; Lefebvre, J.-F.; Kupfer, S.; Gräfe, S.; Demeunynck, M.; Chavarot-Kerlidou, M.; Dietzek, B. Photophysics of a Ruthenium Complex with a π-Extended Dipyridophenazine Ligand for DNA Quadruplex Labeling. *J. Phys. Chem. A* **2018**, *122*, 6558−6569.
(62) Okamoto, T.; Terada, E.; Kozaki, M.; Uchida, M.; Kikukawa, S.; Okada, K. Facile Synthesis of 5,10-Diaryl-5,10-dihydrophenazines and Application to EL Devices. *Org. Lett.* **2003**, *5*, 373−376.
(63) Liu, Q.; Zhao, C.; Tian, G.; Ge, H. Changing Molecular Conjugation with a Phenazine Acceptor for Improvement of Small Molecule-Based Organic Electronic Memory Performance. *RSC Adv.* **2018**, *8*, 805−811.
(64) Day, N. U.; Walter, M. G.; Wamser, C. C. Preparations and Electrochemical Characterizations of Conductive Porphyrin Polymers. *J. Phys. Chem. C* **2015**, *119*, 17378−17388.
(65) Koyama, D.; Dale, H. J. A.; Orr-Ewing, A. J. Ultrafast Observation of a Photoredox Reaction Mechanism: Photoinitiation in Organocatalyzed Atom-Transfer Radical Polymerization. *J. Am. Chem. Soc.* **2018**, *140*, 1285−1293.
(66) Shi, J.; Chen, J.; Chai, Z.; Wang, H.; Tang, R.; Fan, K.; Wu, M.; Han, H.; Qin, J.; Peng, T.; Li, Q.; Li, Z. High Performance Organic Sensitizers Based on 11,12-Bis(hexyloxy)dibenzo[*a*,*c*]phenazine for Dye-Sensitized Solar Cells. *J. Mater. Chem.* **2012**, *22*, 18830−18838.
(67) Richard, C. A.; Pan, Z.; Hsu, H.-Y.; Cekli, S.; Schanze, K. S.; Reynolds, J. R. Effect of Isomerism and Chain Length on Electronic Structure, Photophysics, and Sensitizer Efficiency in Quadrupolar $(Donor)_2$-Acceptor Systems for Application in Dye-Sensitized Solar Cells. *ACS Appl. Mater. Interfaces* **2014**, *6*, 5221−5227.
(68) Huang, Z.-S.; Zang, X.-F.; Hua, T.; Wang, L.; Meier, H.; Cao, D. 2,3-Dipentyldithieno[3,2-f:2′,3′-h]quinoxaline-Based Organic Dyes for Efficient Dye-Sensitized Solar Cells: Effect of π-Bridges and Electron Donors on Solar Cell Performance. *ACS Appl. Mater. Interfaces* **2015**, *7*, 20418−20429.
(69) Murali, M. G.; Wang, X.; Wang, Q.; Valiyaveettil, S. Design and Synthesis of New Ruthenium Complex for Dye-Sensitized Solar Cells. *RSC Adv.* **2016**, *6*, 57872−57879.
(70) Huang, L.; Ma, P.; Deng, G.; Zhang, K.; Ou, T.; Lin, Y.; Wong, M. S. Novel Electron-Deficient Quinoxalinedithienothiophene- and Phenazinedithienothiophene-Based Photosensitizers: The Effect of Conjugation Expansion on DSSC Performance. *Dyes Pigm.* **2018**, *159*, 107−114.
(71) Anderson, H. L. meso-Alkynyl Porphyrins. *Tetrahedron Lett.* **1992**, *33*, 1101−1104.
(72) Arnold, D. P.; Nitschinsk, L. J. Porphyrin Dimers Linked by Conjugated Butadiynes. *Tetrahedron* **1992**, *48*, 8781−8792.
(73) Arnold, D. P.; Manno, D.; Micocci, G.; Serra, A.; Tepore, A.; Valli, L. Porphyrin Dimers Linked by a Conjugated Alkyne Bridge: Novel Moieties for the Growth of Langmuir−Blodgett Films and Their Applications in Gas Sensors. *Langmuir* **1997**, *13*, 5951−5956.
(74) Arnold, D. P.; James, D. A. Dimers and Model Monomers of Nickel(II) Octaethylporphyrin Substituted by Conjugated Groups Comprising Combinations of Triple Bonds with Double Bonds and Arenes. 1. Synthesis and Electronic Spectra. *J. Org. Chem.* **1997**, *62*, 3460−3469.
(75) Maretina, I. A. Porphyrin-Ethynyl Arrays: Synthesis, Design, and Application. *Russ. J. Gen. Chem.* **2009**, *79*, 1544−1581.
(76) Shinokubo, H.; Osuka, A. Marriage of Porphyrin Chemistry with Metal-Catalysed Reactions. *Chem. Commun.* **2009**, 1011−1021.

DOI: 10.1021/acsami.8b20996
ACS Appl. Mater. Interfaces 2019, 11, 8000−8008

(77) Susumu, K.; Therien, M. J. Design of Diethynyl Porphyrin Derivatives with High Near Infrared Fluorescence Quantum Yields. *J. Porphyrins Phthalocyanines* **2015**, *19*, 205−218.
(78) Rickhaus, M.; Vargas Jentzsch, A.; Tejerina, L.; Grübner, I.; Jirasek, M.; Claridge, T. D. W.; Anderson, H. L. Single-Acetylene Linked Porphyrin Nanorings. *J. Am. Chem. Soc.* **2017**, *139*, 16502−16505.
(79) Lu, X.; Fan, S.; Wu, J.; Jia, X.; Wang, Z.-S.; Zhou, G. Controlling the Charge Transfer in D-A-D Chromophores Based on Pyrazine Derivatives. *J. Org. Chem.* **2014**, *79*, 6480−6489.
(80) Higashino, T.; Imahori, H. Porphyrins as Excellent Dyes for Dye-Sensitized Solar Cells: Recent Developments and Insights. *Dalton Trans.* **2015**, *44*, 448−463.
(81) Zhang, C.-R.; Li, X.-Y.; Shen, Y.-L.; Wu, Y.-Z.; Liu, Z.-J.; Chen, H.-S. Molecular Docking toward Panchromatic Dye Sensitizers for Solar Cells Based upon Tetraazulenylporphyrin and Tetraanthracenylporphyrin. *J. Phys. Chem. A* **2017**, *121*, 2655−2664.
(82) Takanami, T.; Wakita, A.; Sawaizumi, A.; Iso, K.; Onodera, H.; Suda, K. One-Pot Synthesis of *meso*-Formylporphyrins by S_NAr Reaction of 5,15-Disubstituted Porphyrins with (2-Pyridyldimethylsilyl)methyllithium. *Org. Lett.* **2008**, *10*, 685−687.
(83) Yu, L.; Muthukumaran, K.; Sazanovich, I. V.; Kirmaier, C.; Hindin, E.; Diers, J. R.; Boyle, P. D.; Bocian, D. F.; Holten, D.; Lindsey, J. S. Excited-State Energy-Transfer Dynamics in Self-Assembled Triads Composed of Two Porphyrins and an Intervening Bis(dipyrrinato)metal Complex. *Inorg. Chem.* **2003**, *42*, 6629−6647.
(84) Lindsey, J. S.; Wagner, R. W. Investigation of the Synthesis of Ortho-Substituted Tetraphenylporphyrins. *J. Org. Chem.* **1989**, *54*, 828−836.
(85) Sheridan, M. V.; Lam, K.; Geiger, W. E. Covalent Attachment of Porphyrins and Ferrocenes to Electrode Surfaces through Direct Anodic Oxidation of Terminal Ethynyl Groups. *Angew. Chem., Int. Ed.* **2013**, *52*, 12897−12900.
(86) High, J. S.; Virgil, K. A.; Jakubikova, E. Electronic Structure and Absorption Properties of Strongly Coupled Porphyrin-Perylene Arrays. *J. Phys. Chem. A* **2015**, *119*, 9879−9888.
(87) Koenigsmann, C.; Ripolles, T. S.; Brennan, B. J.; Negre, C. F. A.; Koepf, M.; Durrell, A. C.; Milot, R. L.; Torre, J. A.; Crabtree, R. H.; Batista, V. S.; Brudvig, G. W.; Bisquert, J.; Schmuttenmaer, C. A. Substitution of a Hydroxamic Acid Anchor into the MK-2 Dye for Enhanced Photovoltaic Performance and Water Stability in a DSSC. *Phys. Chem. Chem. Phys.* **2014**, *16*, 16629−16641.
(88) Sawyer, D. T.; Sobkowiak, A.; Roberts, J. L., Jr. *Electrochemistry for Chemists*, 2nd ed.; John Wiley & Sons, Inc.: New York, 1995.
(89) Becke, A. D. Density-Functional Thermochemistry. III. The Role of Exact Exchange. *J. Phys. Chem.* **1993**, *98*, 5648−5652.
(90) Weigend, F.; Ahlrichs, R. Balanced Basis Sets of Split Valence, Triple Zeta Valence and Quadruple Zeta Valence Quality for H to Rn: Design and Assessment of Accuracy. *Phys. Chem. Chem. Phys.* **2005**, *7*, 3297−3305.
(91) Frisch, M. J.; Trucks, G. W.; Schlegel, H. B.; Scuseria, G. E.; Robb, M. A.; Cheeseman, J. R.; Scalmani, G.; Barone, V.; Mennucci, B.; Petersson, G. A.; Nakatsuji, H.; Caricato, M.; Li, X.; Hratchian, H. P.; Izmaylov, A. F.; Bloino, J.; Zheng, G.; Sonnenberg, J. L.; Hada, M.; Ehara, M.; Toyota, K.; Fukuda, R.; Hasegawa, J.; Ishida, M.; Nakajima, T.; Honda, Y.; Kitao, O.; Nakai, H.; Vreven, T.; Montgomery, J. A., Jr.; Peralta, J. E.; Ogliaro, F.; Bearpark, M.; Heyd, J. J.; Brothers, E.; Kudin, K. N.; Staroverov, V. N.; Kobayashi, R.; Normand, J.; Raghavachari, K.; Rendell, A.; Burant, J. C.; Iyengar, S. S.; Tomasi, J.; Cossi, M.; Rega, N.; Millam, J. M.; Klene, M.; Knox, J. E.; Cross, J. B.; Bakken, V.; Adamo, C.; Jaramillo, J.; Gomperts, R.; Stratmann, R. E.; Yazyev, O.; Austin, A. J.; Cammi, R.; Pomelli, C.; Ochterski, J. W.; Martin, R. L.; Morokuma, K.; Zakrzewski, V. G.; Voth, G. A.; Salvador, P.; Dannenberg, J. J.; Dapprich, S.; Daniels, A. D.; Farkas, Ö.; Foresman, J. B.; Ortiz, J. V.; Cioslowski, J.; Fox, D. J. *Gaussian 09*; Gaussian, Inc.: Wallingford CT, 2009.
(92) Furche, F.; Ahlrichs, R. Adiabatic Time-Dependent Density Functional Methods for Excited State Properties. *J. Chem. Phys.* **2002**, *117*, 7433−7447.
(93) Marenich, A. V.; Cramer, C. J.; Truhlar, D. G. Universal Solvation Model Based on Solute Electron Density and on a Continuum Model of the Solvent Defined by the Bulk Dielectric Constant and Atomic Surface Tensions. *J. Phys. Chem. B* **2009**, *113*, 6378−6396.
(94) Martin, R. L. Natural Transition Orbitals. *J. Chem. Phys.* **2003**, *118*, 4775−4777.

DOI: 10.1021/acsami.8b20996
ACS Appl. Mater. Interfaces 2019, 11, 8000−8008